EXPLOSIVE SAFETY COMPLIANCE OF A WEAPON ASSEMBLY OPERATION

By:

Mohsen Sanai and Gary Greenfield

SRI International
333 Ravenswood Avenue
Menlo Park, CA 94025

DoD Explosives Safety Seminar
St. Louis, Missouri
August 28-30, 1990

Report Documentation Page

Form Approved
OMB No. 0704-0188

1. REPORT DATE	2. REPORT TYPE	3. DATES COVERED
AUG 1990		**00-00-1990 to 00-00-1990**

4. TITLE AND SUBTITLE	5a. CONTRACT NUMBER
Explosive Safety Compliance of a Weapon Assembly Operation	5b. GRANT NUMBER
	5c. PROGRAM ELEMENT NUMBER
6. AUTHOR(S)	5d. PROJECT NUMBER
	5e. TASK NUMBER
	5f. WORK UNIT NUMBER
7. PERFORMING ORGANIZATION NAME(S) AND ADDRESS(ES) **SRI International,333 Ravenswood Avenue,Menlo Park,CA,94025**	8. PERFORMING ORGANIZATION REPORT NUMBER
9. SPONSORING/MONITORING AGENCY NAME(S) AND ADDRESS(ES)	10. SPONSOR/MONITOR'S ACRONYM(S)
	11. SPONSOR/MONITOR'S REPORT NUMBER(S)

12. DISTRIBUTION/AVAILABILITY STATEMENT
Approved for public release; distribution unlimited

13. SUPPLEMENTARY NOTES
See also ADA235005, Volume 1. Minutes of the Explosives Safety Seminar (24th) Held in St. Louis, MO on 28-30 August 1990.

14. ABSTRACT

15. SUBJECT TERMS

16. SECURITY CLASSIFICATION OF:			17. LIMITATION OF ABSTRACT	18. NUMBER OF PAGES	19a. NAME OF RESPONSIBLE PERSON
a. REPORT	b. ABSTRACT	c. THIS PAGE			
unclassified	**unclassified**	**unclassified**	**Same as Report (SAR)**	**31**	

CONTENTS

ILLUSTRATIONS

ILLUSTRATIONS (Continued)

INTRODUCTION

SRI International evaluated the explosive operations of a weapons assembly operation to determine compliance with the U.S. Department of Defense (DoD) quantity/distance (Q/D) requirements for blast overpressure and fragment projection distance. Figure 1 shows a schematic of the weapon assembly and inhabited buildings. The closest distance between the two buildings (for later use with Q/D charts) is 550 ft.

Our objective was to obtain a credible estimate of the hazardous overpressure range and fragment projection range should an accidental explosion (or "maximum credible event") occur in the weapon assembly building. The estimated hazardous ranges can then be compared with the 550-ft separation between the two buildings. The range estimates given here are based on computer simulation of mass detonation of an equivalent high explosive (HE) charge. The hydrocode calculations model the HE detonation, the formation and propagation of the resulting airblast, and the initial velocity imparted to fragments of known material and mass. A special algorithm (called UFO) was developed to trace the fragment trajectories and calculate the maximum projection distance possible for a given fragment mass and initial speed.

The maximum amount of explosive and propellant in use in the weapon assembly operation at any given time was calculated from a combination of rocket motors, warheads, and complete weapons stored in several locations. The total equivalent HE for the entire weapon assembly operation is about 2450 lb. Thus, for the 6650 ft^2 weapon assembly building, the average explosive loading density is 0.37 lb/ft^2. This loading density is used in the blast overpressure and fragment projection distance calculations discussed in the following sections.

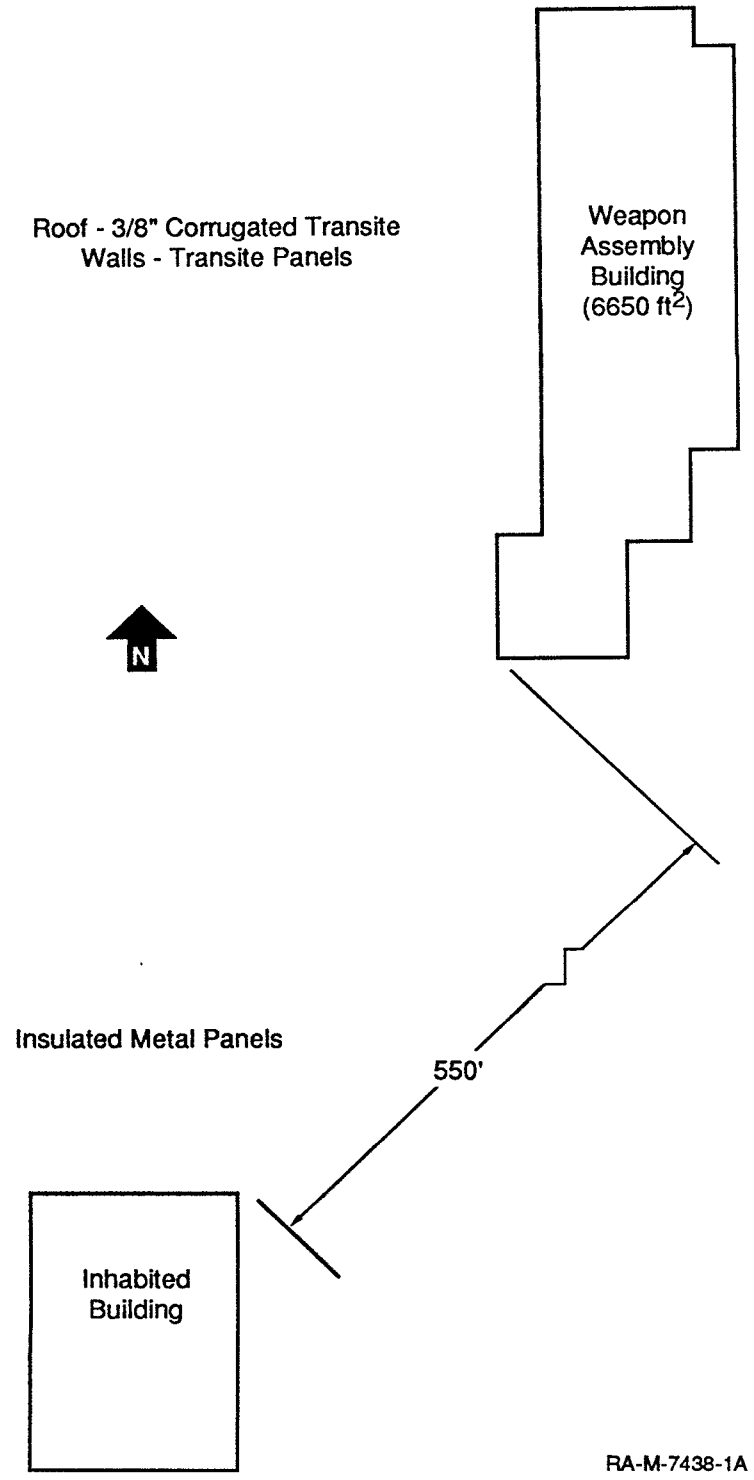

Figure 1. Relative locations of assembly and inhabited buildings.

BLAST OVERPRESSURE

To calculate the maximum blast overpressure that could occur at the inhabited building, we modeled the mass detonation of the equivalent HE charge in the weapon assembly building using the SRI two-dimensional L2D Lagrangian hydrocode. Figure 2 shows the overall computer zone layout used in this calculation, and Figure 3 shows an enlarged view of the central section.The outer concrete walls are modeled as rigid; the much weaker blowout roof is not included in the calculation so that the calculation of pressures is conservative (upper bound). The assembly building is modeled as a 46-ft-radius cylindrical chamber with a cross sectional area of 6650 ft^2 equal to the floor area of the actual assembly building shown in Figure 1. TNT explosive is assumed to be distributed uniformly on the floor, and its detonation is modeled by a standard JWL equation of state.

Figure 4 shows the constant-pressure (isobar) contours 5 ms after the HE is detonated. The pressure contours show that at this early time the flow near the center is moving upward and the flow near the edge is spilling over the outside wall. The numbers on each pressure contour signify the pressure level. Number 1 indicates a pressure of 1 bar and number 8 a pressure of 8 bar. The pressure contours are closer to each other near the outer region of the flow, indicating the presence of an expanding shock wave in air with a peak overpressure of about 100 psi at this time.

Figure 5 shows the calculated peak overpressures as the blast reaches the vicinity of the inhabited building. The overpressures are plotted versus the standoff distance measured from the edge of the weapon assembly building so that it can be compared directly with the 550-ft standoff distance between the two buildings. This plot shows that the expected peak blast overpressure at the inhabited building is about 0.3 psi, which is significantly lower than the maximum allowable overpressure level of 1.2 psi specified in the DoD safety manual. The results of the calculations clearly show that the DoD blast overpressure standard for inhabited buildings is amply satisfied for the 2456-lb HE capacity of the weapon assembly building.

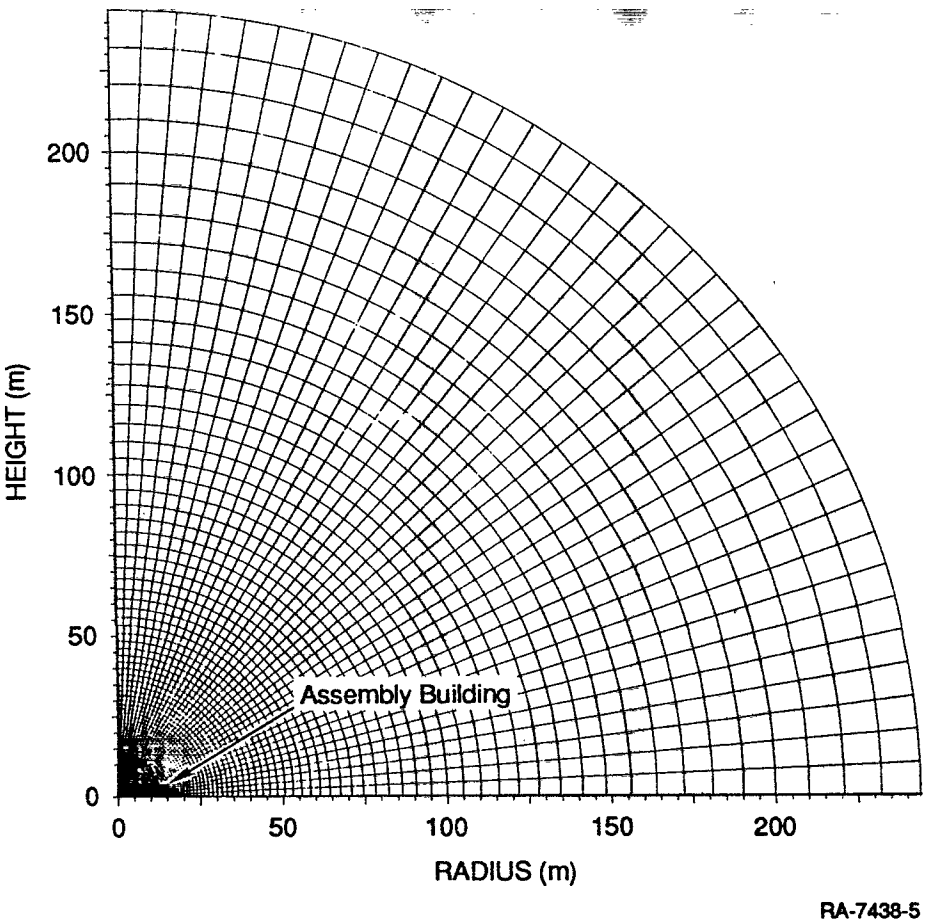

Figure 2. Computer zone layout for airblast calculations.

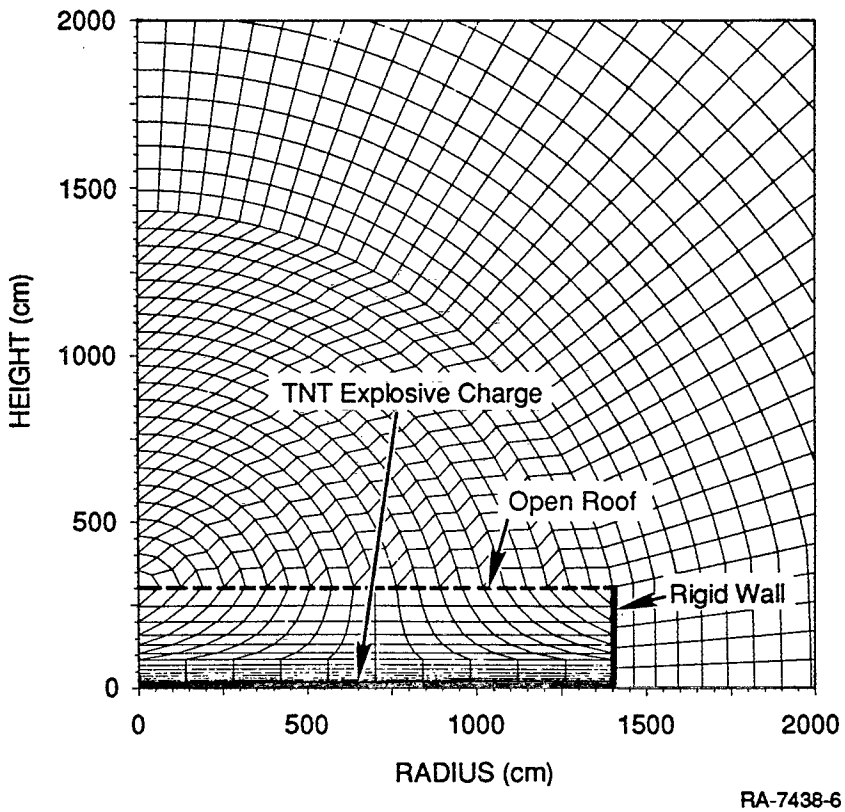

Figure 3. Exploded view of computer zone layout for airblast calculations.

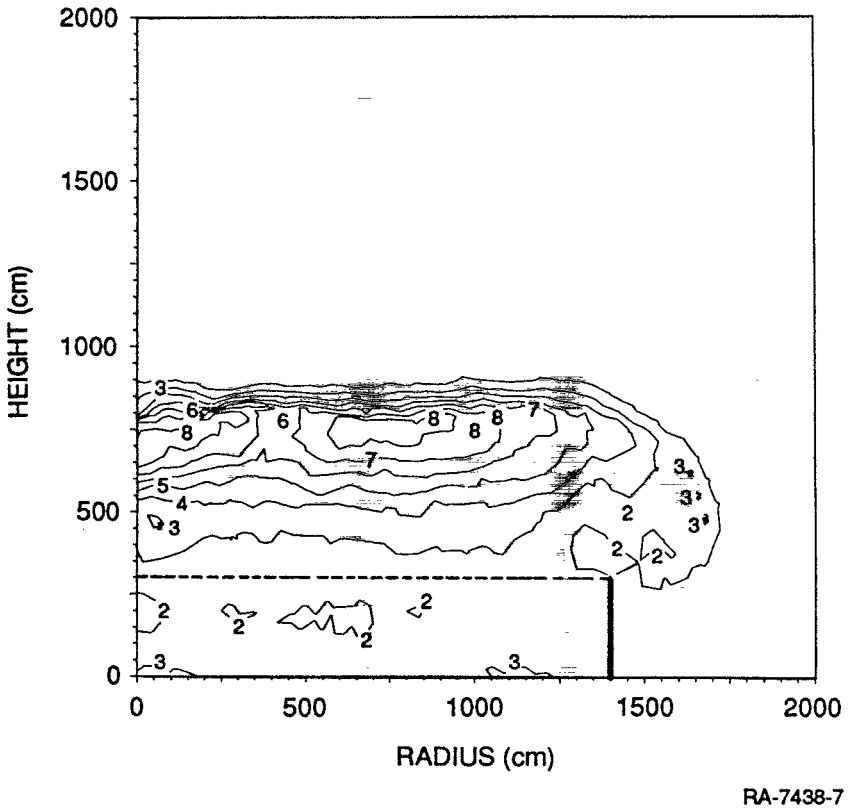

Figure 4. Pressure contours 5 ms after explosive charge initiation.

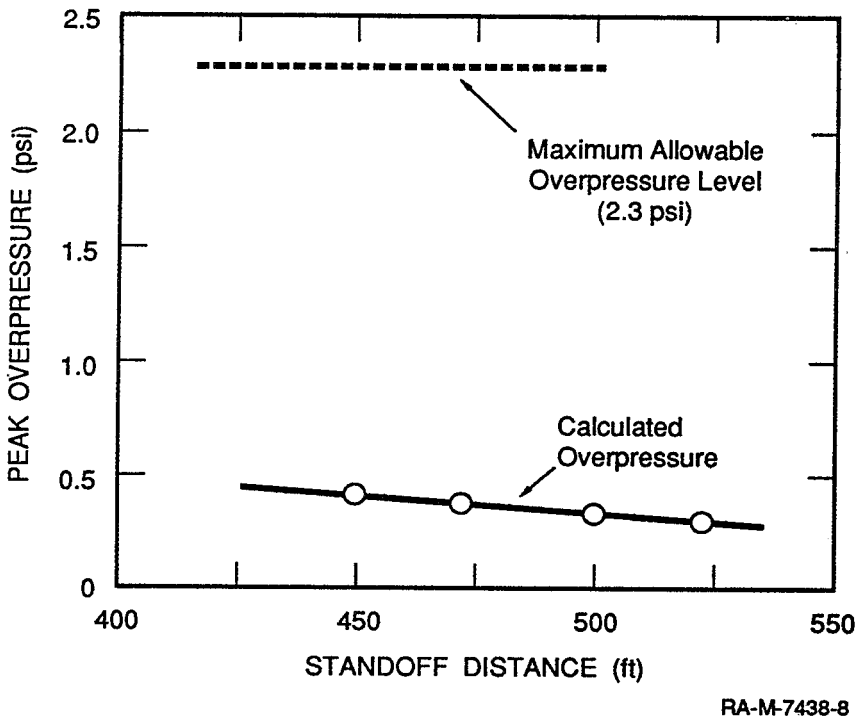

Figure 5. Variation of airblast overpressure with standoff distance from the weapon assembly building.

FRAGMENT VELOCITIES AND DIMENSIONS

To calculate the hazardous fragment ranges, we need to estimate not only the initial velocity but also the expected dimensions (or mass) of each fragment. As will be seen in the next section, this velocity and mass information is used in the UFO algorithm to calculate the maximum projection distance for any projection angle.

FRAGMENT VELOCITIES

We identified two major sources of fragments and debris in the event of an accidental explosion in the weapon assembly building. They are (1) fragments produced by the rupture of the steel casing of the weapon round and (2) fragments produced by the roof material due to explosive detonation. In each case, the fragment velocity is determined based on a series of hydrocode calculations similar to those used to calculate the blast overpressure in the previous section.

Figure 6 shows the idealized axisymmetric model used for the weapon casing in the hydrocode calculations. The model is based on the height, diameter, and total weight of the actual weapon. The equivalent TNT weight obtained above is modeled as an HE cylinder with a radius of 2.1 cm. A steel shell surrounds the HE. As the HE is detonated, the steel shell is expanded and fragmented into long narrow strips. Because the present one-dimensional calculation neglects the strength of the shell and the expansion of explosive products from the two ends of the weapon casing, it provides a conservative (higher) estimate of the projection velocity for the fragments (steel shell).

The calculated time history of the steel shell is shown by the solid curve in Figure 7. The shell is accelerated rapidly and reaches its limiting velocity of 1750 m/s about 80 μs after charge initiation at zero time. The dashed curve lying below the solid curve in Figure 7 is the shell velocity calculated from a two-dimensional hydrocode calculation in which the shell was assumed to be fragmented into 0.2-cm-wide strips. As the shell expands, the explosive products escape through the widening gaps between neighboring fragments, thus imparting less momentum (and velocity) to the fragments. Again, to be conservative, we used the maximum velocity of 1750 m/s calculated from the one-dimensional calculations (solid curve in Figure 7) as the projection velocity for the fragments produced by the weapon casing.

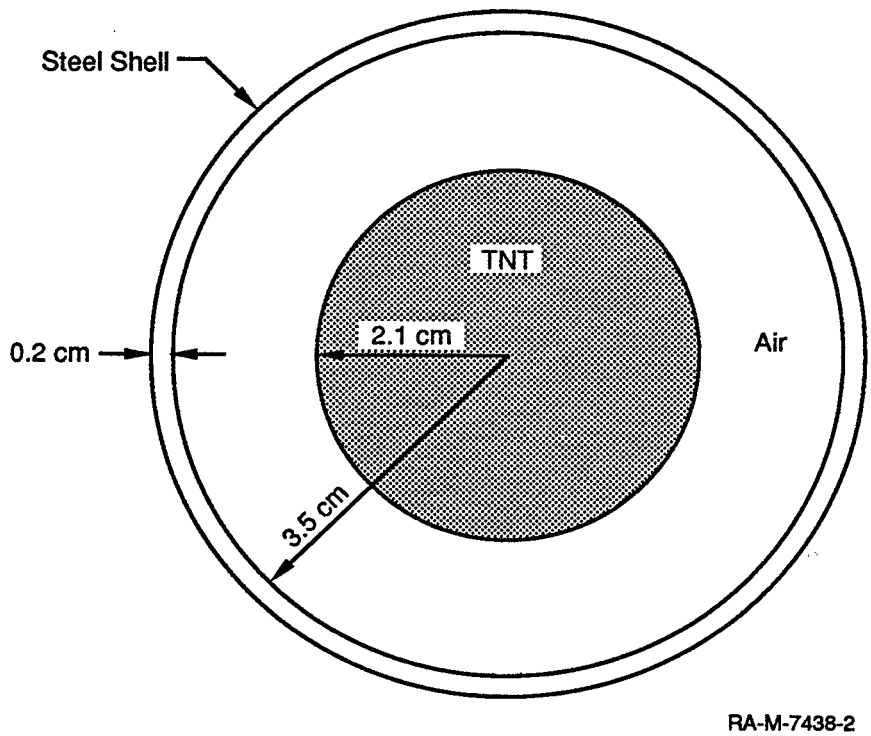

Figure 6. Model of weapon round used in hydrocode calculations performed to estimate maximum projection velocity of steel shell fragments.

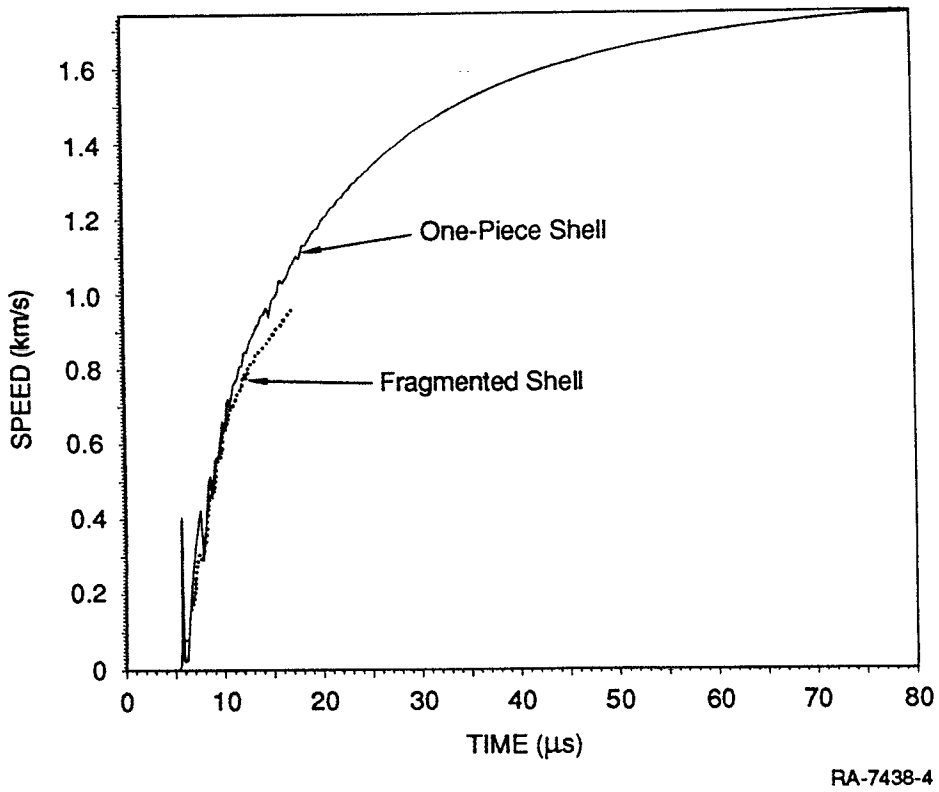

Figure 7. Calculated projection velocity of steel shell fragments.

To calculate the roof fragment velocity, we used the idealized one-dimensional model shown in Figure 8. As before, the calculations provide a conservative (higher) estimate of the projection velocity because the effect of gas escape through fragmented roof panels is neglected. Note that the total explosive areal density calculated above is used here without any downward adjustment of the HE weight due to the explosive energy converted into the kinetic energy of the weapon casing. (Based on the calculated casing velocity of 1750 m/s, the kinetic energy of the casing is over 30% of the total explosive energy.) The kinetic energy imparted to the weapon casing clearly reduces the intensity of the shock wave responsible for projecting the roof material, so the present calculations should result in a conservative (higher) estimate of fragment velocities.

The idealized model shown in Figure 8 is based on the manufacturer's specifications for corrugated "400" sheets. The average thickness of the panels is 3/8 in., but we used a .5-in.-thick (1.27-cm) panel in the calculations to account for the extra weight per unit area due to the corrugation. The maximum velocity of the roof panels obtained from this calculation was 383 m/s.

FRAGMENT DIMENSIONS

The weapon casing and roof panels are expected to fragment into long narrow strips and be projected in arbitrary directions following an accidental explosion. These strips can be as long as the undamaged unit: 4 ft for the weapon casing and 6 ft for the roof panels. The nominal widths of these strips can be obtained from the standard Mott theory discussed in References 1 and 2. According to this theory, the nominal fragment size is determined by the competition between the momentum diffusion velocity and the loading rate.

Straightforward application of Mott's theory resulted in nominal widths of 0.2 cm and 1.78 cm for the weapon casing and roof panels, respectively. (As expected, these values are comparable to the original thicknesses of the weapon casing and roof panels.) To account for the statistical variation of fragment widths, we made the assumption that the maximum fragment width can be as much as three times greater than the nominal value calculated based on Mott's theory. In accordance with the available literature on fragmentation of bomb casings, we believe this assumption leads to a reasonably conservative (high) estimate of fragment widths.

The nominal fragment weights calculated using Mott's theory are 38.1 g and 669 g for the weapon casing and roof panels, respectively. The maximum values used in the UFO calculations (discussed in the next section) are 114 g and 1970 g, three times larger than the nominal values.

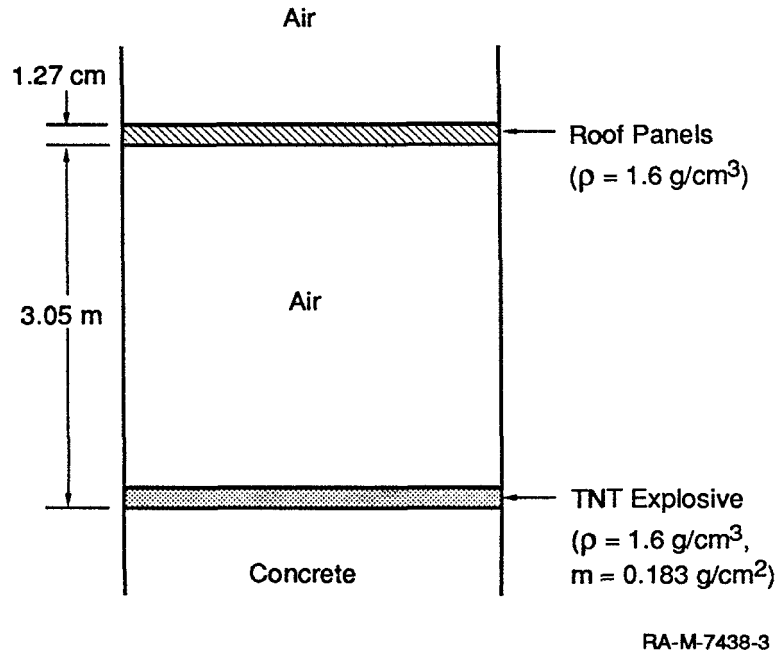

Figure 8. Model of weapon assembly building used in hydrocode calculations to estimate maximum projection velocity of roof panel fragments.

FRAGMENT PROJECTION DISTANCES

To calculate the fragment projection distances, we wrote a computer algorithm (called UFO) that calculates possible trajectories for a fragment with known weight and initial speed. As shown in Figure 9, the trajectory of a fragment in free flight depends only on its weight, Mg, and air drag, F_D. Based on Newton's Law, fragment acceleration in the horizontal and vertical directions is given by the formuli in Figure 9, where C_D is the drag coefficient and A_D is the projected area of the fragment on a surface perpendicular to the flight trajectory. Once the values of C_D and A_D are determined, the UFO calculates possible trajectories by changing the initial projection angle from 0 to 90 at one-degree intervals. The UFO algorithm is validated in the Appendix, where its results are shown to be consistent with known analytic trajectories as well as with the results of a similar algorithm discussed in References 3 and 4.

Realistic estimates of C_D and A_D are needed to calculate the maximum projection distances. Both C_D and A_D change continuously as the fragment tumbles in flight. The fragments of interest are in the form of long strips. Figure 10 shows three extreme flight orientations for a strip fragment and the corresponding drag coefficients and projection areas. (Projected areas are shaded in Figure 10.) We simply averaged the drag coefficients and projected areas of the three extreme flight orientations shown in Figure 10. This should give representative values for C_D and A_D for the UFO calculations.

Results of UFO calculations for the weapon casing and roof panels are shown in Figures 11 through 14. Each figure shows the flight trajectory obtained for 17 projection angles ranging from 5 to 85 degrees at 5-degree intervals. Figures 11 and 13 show the trajectories obtained with nominal fragment weights obtained from Mott's theory. The maximum projection distances obtained for the weapon casing and roof panels are 351 ft and 400 ft, respectively. These results show that the hazardous range for nominal-size fragments is less than 400 ft, irrespective of the orientation at which they are projected. Similar calculations shown in Figures 12 and 14 for the largest fragments (three times the nominal widths) indicate that the hazardous ranges are increased to 528 ft and 525 ft for the weapon casing and roof panels, respectively.

The estimates of fragment weights and speeds are generally conservative (i.e., resulting in maximal values). With the several conservative assumptions included, we calculate that the hazardous range for fragments is smaller than the 550-ft separation between the weapons assembly and inhabited buildings.

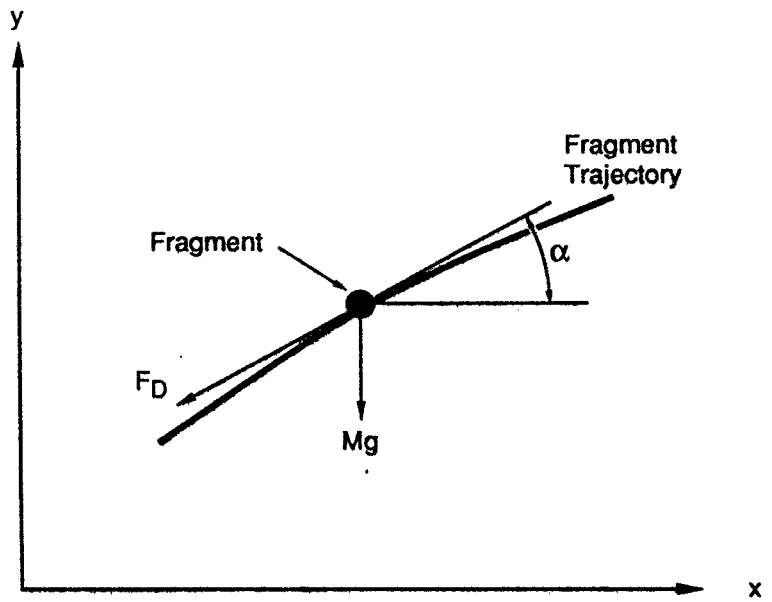

$$F_D = 1/2\ \rho\ C_D A_D\ (\dot{x}^2 + \dot{y}^2)$$

$$\ddot{x} = -\frac{F_D \cos\alpha}{M}$$

$$\ddot{y} = -\frac{F_D \sin\alpha}{M} - g$$

RA-M-7438-14

Figure 9. Formulas used in SRI UFO algorithm to calculate fragment trajectory and projection distance.

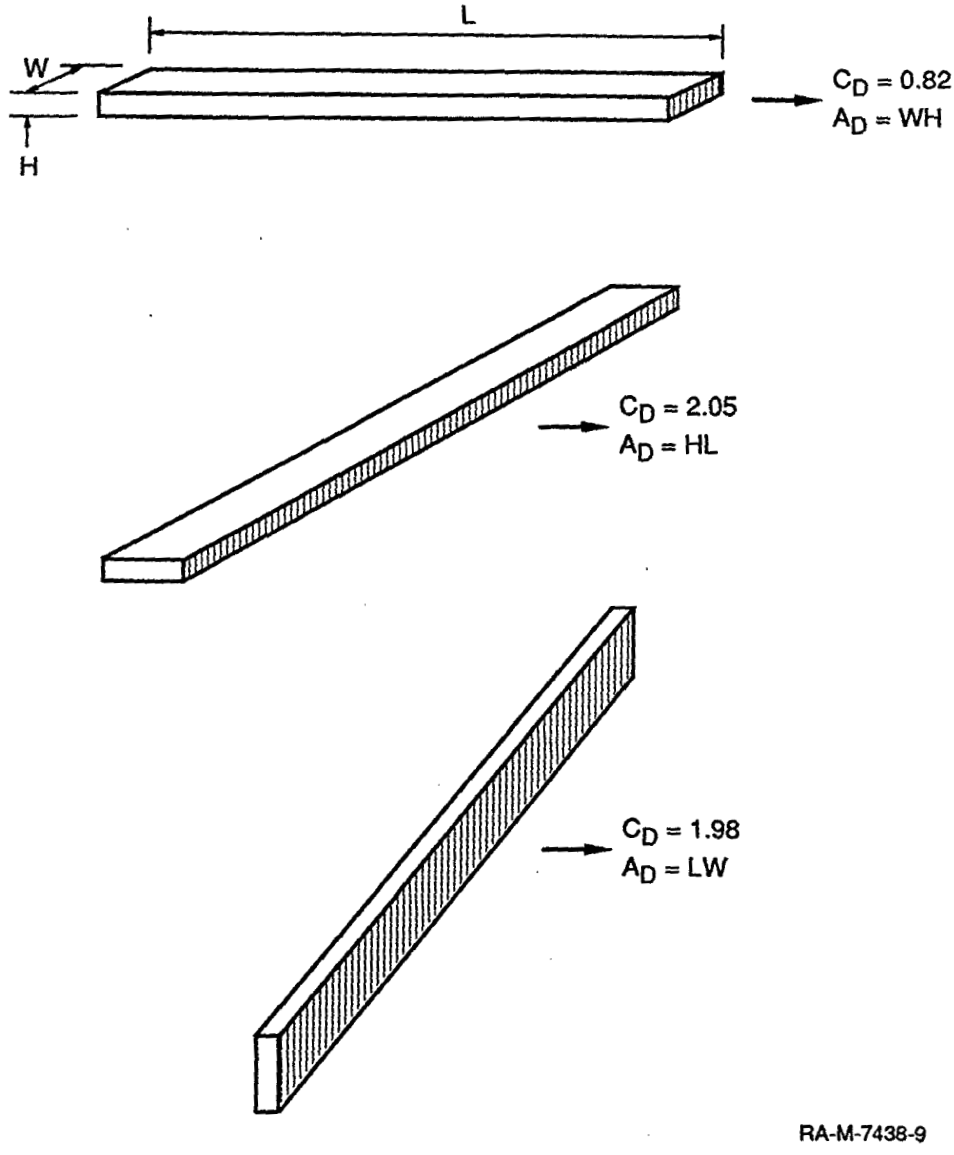

Figure 10. Drag coefficients for strips (Refs. 3 and 4).

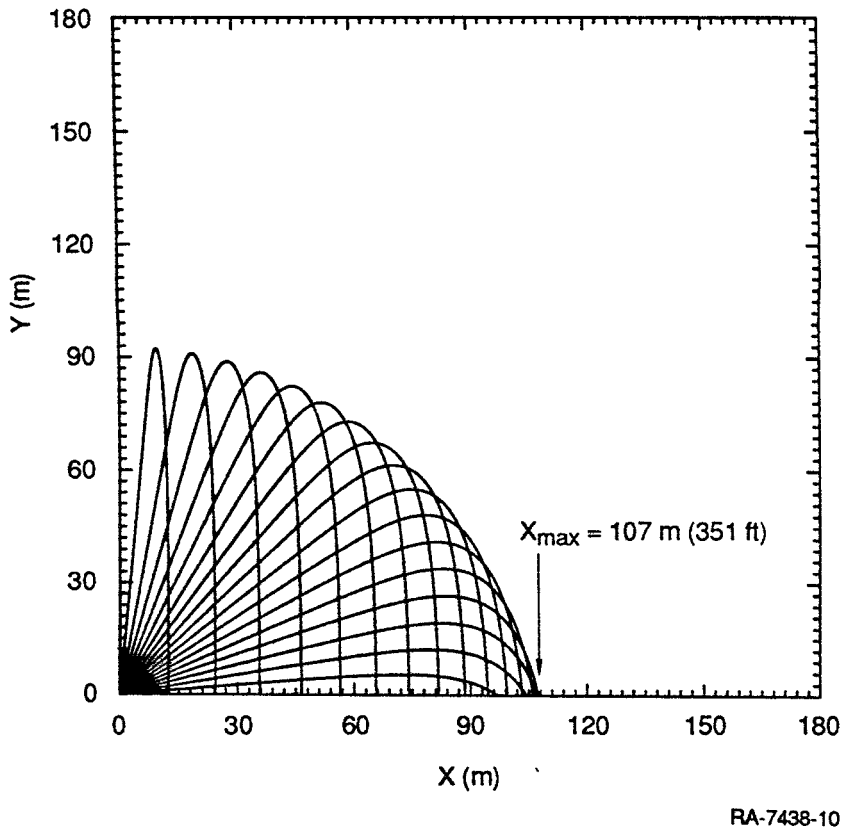

Figure 11. Projection distances calculated for a 0.2-cm-wide, 1.2-m-long steel shell fragment.

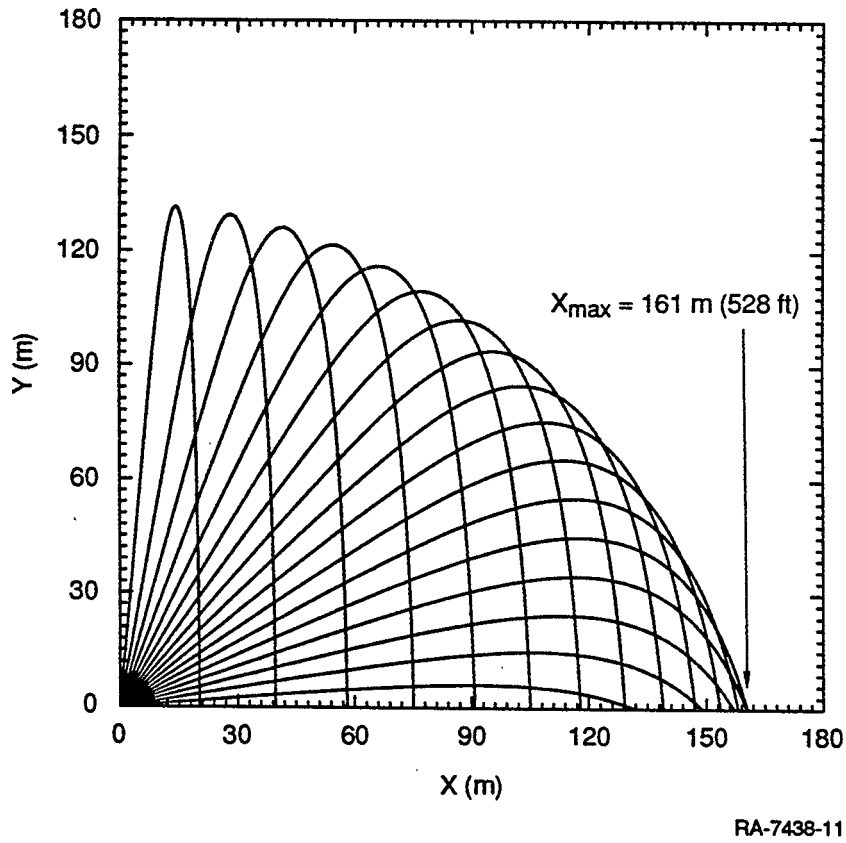

Figure 12. Projection distances calculated for a 0.6-cm-wide, 1.2-m-long steel shell fragment.

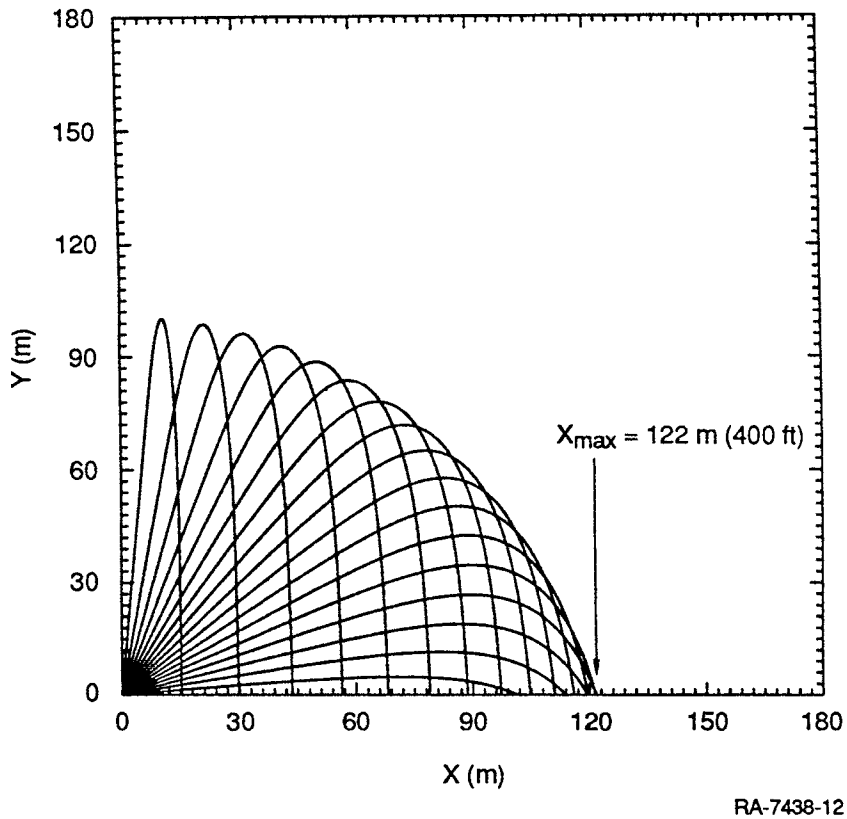

Figure 13. Projection distances calculated for a 1.8-cm-wide, 1.8-m-long roof panel fragment.

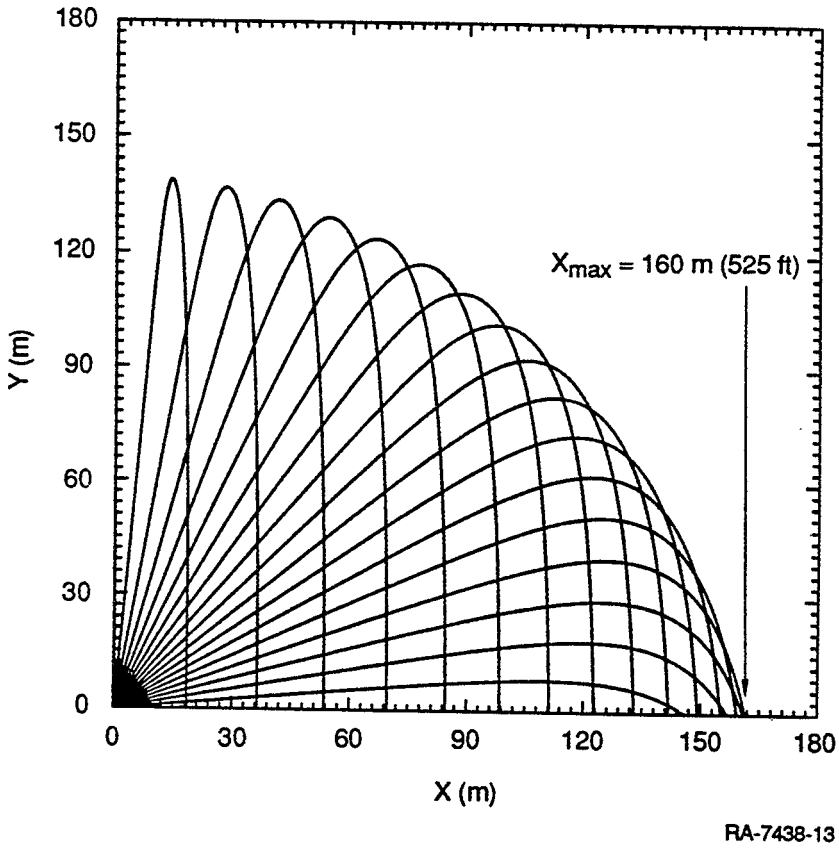

Figure 14. Projection distances calculated for a 5.3-cm-wide, 1.8-m-long roof panel fragment.

CONCLUSIONS

The results of the computer simulation and fragment trajectory calculations discussed in this report show that the 550-ft distance between the inhabited building and the weapon assembly operation is consistent with the safety guidelines provided in the DoD manual for peak blast overpressure and hazardous fragment range. In particular, these calculations have shown that an accidental mass detonation of an equivalent HE charge (2456 lb of TNT) will result in a peak blast overpressure at the inhabited building of about 0.5 psi, which is much less than the 1.2 psi allowed under the current regulations. In addition, calculations performed for fragments produced from the weapon casing and roof panels indicate that the nominal fragment hazardous range is 400 ft and the maximum range is 528 ft, both less than the 550-ft separation between the two buildings.

REFERENCES

(1) N. F. Mott, Proc. R. Soc. Lond. A **189**, 300-308 (1947).

(2) D. E. Grady and M. E. Klipp, J. Mech. Phys. Solids **35**(1), 95-118 (1987).

(3) W. E. Baker et al., "Workbook for Estimating Effects of Accidental Explosions in Propellant Ground Handling and Transport Systems," NASA Contractor Report 3023, Contract NAS3-20497 (August 1978).

(4) W. E. Baker et al., "Explosion Hazards and Evaluation," Fundamental Studies in Engineering **5** (1983).

APPENDIX

UFO ALGORITHM FOR CALCULATING FRAGMENT PROJECTION DISTANCES

To calculate the fragment projection distances, we wrote a computer algorithm (called UFO) that calculates all the possible trajectories for a fragment with known weight and initial speed. As shown in Figure 9 above, the trajectory of a fragment in free flight depends only on its weight, Mg, and air drag, F_D. Based on Newton's Law, fragment acceleration in the horizontal and vertical directions is given by the formuli in Figure 9, where C_D is the drag coefficient and A_D is the projected area of the fragment on a surface perpendicular to the flight trajectory. Once the values of C_D and A_D are determined, the UFO calculates possible trajectories by changing the initial projection angle from 0 to 90 at one-degree intervals.

We validated the UFO algorithm by comparing it with the classic case of a free flying projectile in vacuum (no air drag). As shown in Figure A-1, the flight trajectory is a parabola for this case. For the projection angle of 45 degrees used in the present calculation, the maximum range should be four times larger than the maximum height, which is seen to be the case in Figure A-1.

Figure A-2 shows how the orientation of the flight trajectory changes with projection distance. The orientation angle changes from +45 degrees to -45 degrees at the initial and final intersections of the flight trajectory with the horizontal ground plane. The orientation angle of zero corresponds to when the projectile has reached its maximum height. As shown in Figure A-3, the kinetic energy of the projectile at this point reaches its minimum value and the potential energy of the projectile (projectile weight times its height above the ground plane) reaches its maximum value.

The UFO algorithm was further validated by comparing it with a similar code discussed in References 3 and 4. Over 5000 UFO calculations were performed to generate the universal curve shown in Figure A-4(a). Every main parameter that influence the maximum projection distance was changed in small steps over a range extending at least one order of magnitude. The parameters included were the drag coefficient, fragment weight, initial speed, and projected area. For each combination of these parameters, the maximum fragment projection distance was calculated by changing the projection angles from 5 to 85 degrees at small intervals. The maximum nondimensional projection distance R [ordinate in Figure A-4(a)] was then plotted against

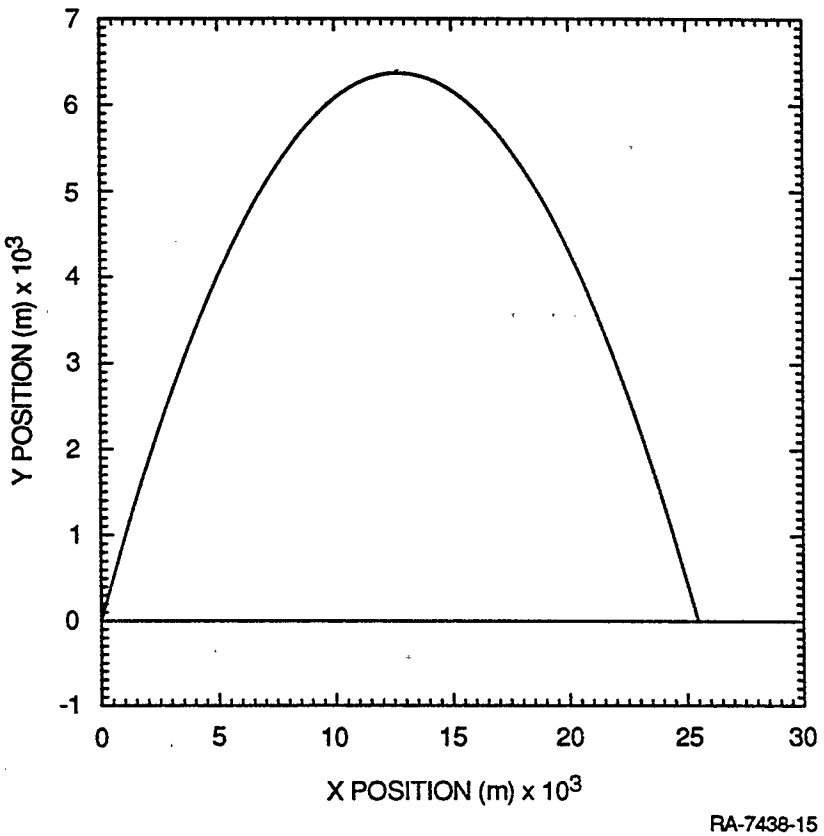

Figure A-1. Trajectory calculation to check SRI UFO algorithm ($C_D = 0$, $\alpha = 45°$).

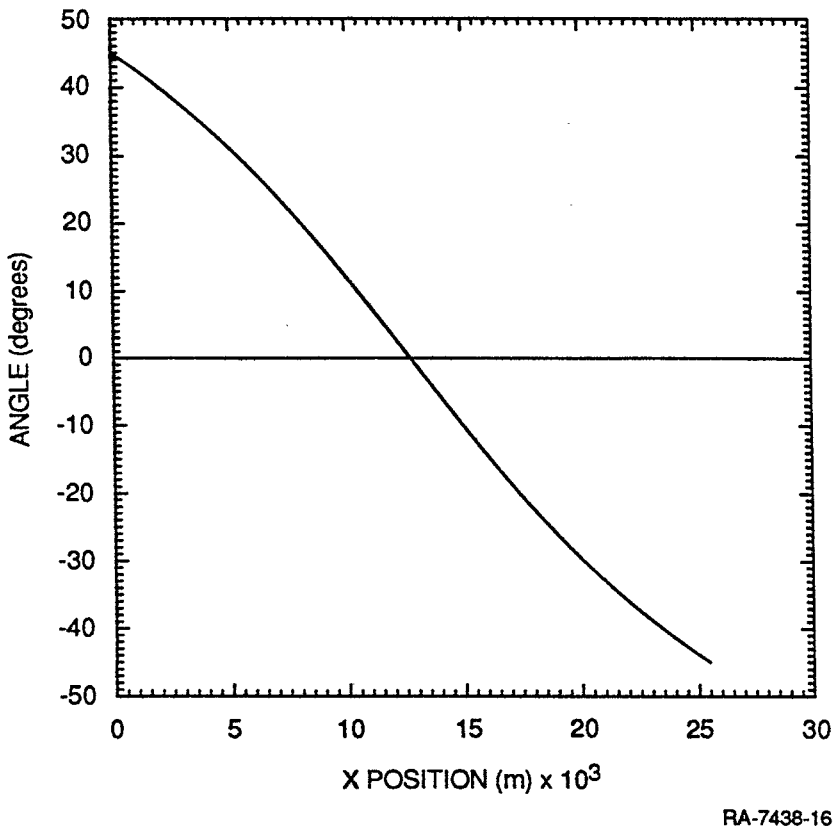

Figure A-2. Variation of trajectory angle with distance ($C_D = 0$, $\alpha = 45°$).

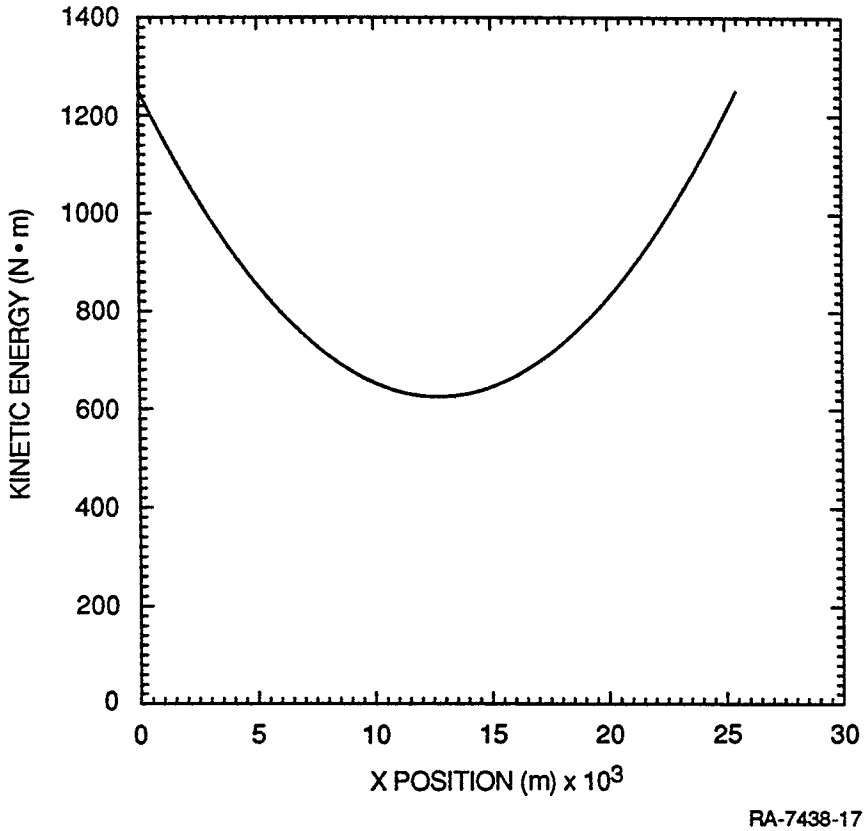

Figure A-3. Variation of fragment kinetic energy with distance ($C_D = 0$, $\alpha = 45°$).

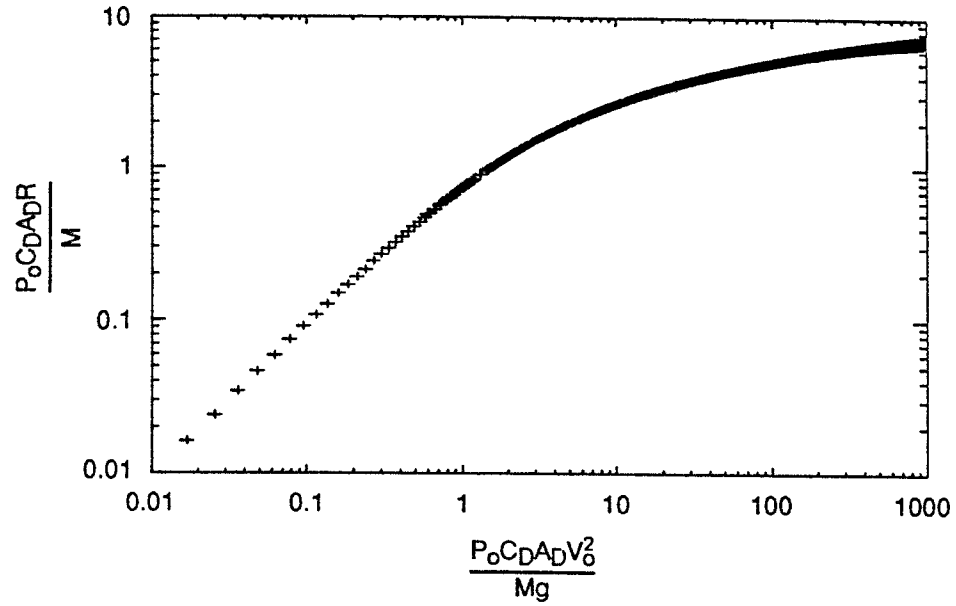

(a) SRI UFO calculation

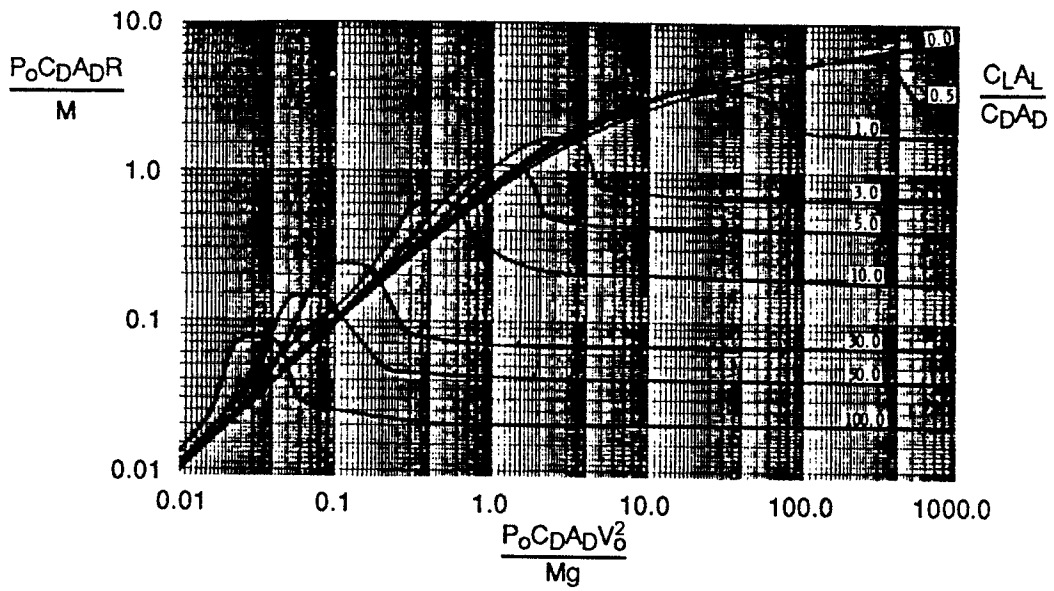

(b) NASA FRISBEE calculations (Ref. 3)

RA-7438-18

Figure A-4. Fragment maximum projection distances predicted by NASA FRISBEE and SRI UFO algorithms.

another nondimensional parameter that includes the square of the initial projectile speed. The UFO algorithm predicts that the nondimensionalized range increases monotonically with the initial speed and approaches a plateau of 10.

Results of similar calculations reported in Reference 3 are shown in Figure A-4(b). If superimposed, the central curve that is marked 0.0 exactly overlays the UFO curve. This 0.0 number signifies the ratio of the lift to drag coefficients, which is assumed to be zero for the UFO calculations. Incidentally, note that the calculations with finite drag coefficients result in a smaller projection distance, indicating that the assumption of zero lift coefficients made in the UFO results in conservative (greater) fragment projection distances.